

Short-Period Strain (0.1–10⁵ s): Near-Source Strain Field for an Earthquake (M_L 3.2) Near San Juan Bautista, California

M. J. S. JOHNSTON AND R. D. BORCHERDT

U.S. Geological Survey, Menlo Park, California

A. T. LINDE

Carnegie Institution of Washington, Washington, D. C.

Measurements of dilational earth strain in the frequency band 25–10⁻⁵ Hz have been made on a deep borehole strainmeter installed near the San Andreas fault. These data are used to determine seismic radiation fields during nuclear explosions, teleseisms, local earthquakes, and ground noise during seismically quiet times. Strains of less than 10⁻¹⁰ on these instruments can be clearly resolved at short periods (< 10 s) and are recorded with wide dynamic range digital recorders. This permits measurement of the static and dynamic strain variations in the near field of local earthquakes. Noise spectra for earth strain referenced to 1 (strain)²/Hz show that strain resolution decreases at about 10 dB per decade of frequency from -150 dB at 10⁻⁴ Hz to -223 dB at 10 Hz. Exact expressions are derived to relate the volumetric strain and displacement field for a homogeneous *P* wave in a general viscoelastic solid as observed on collocated dilatometers and seismometers. A rare near-field recording of strain and seismic velocity was obtained on May 26, 1984, from an earthquake (M_L 3.2) at a hypocentral distance of 3.2 km near the San Andreas fault at San Juan Bautista, California. While the data indicate no precursory strain release at the 5 × 10⁻¹¹ strain level, a coseismic strain release of 1.86 nanostrain was observed. This change in strain is consistent with that calculated from a simple dislocation model of the event. Ground displacement spectra, determined from the downhole strain data and instrument-corrected surface seismic data, suggest that source parameters estimated from surface recordings may be contaminated by amplification effects in near-surface low-velocity materials.

INTRODUCTION

Borehole strain sensors installed at depths between 100 and 200 m can detect strains at levels at least 20 dB below those obtained on near-surface strainmeters [Johnston *et al.*, 1982; Johnston and Borchardt, 1984] with a dynamic range exceeding 100 dB [Sacks *et al.*, 1971; Sacks, 1979; Gladwin, 1984] over a period band of 0.1 s to several months. The wide dynamic range and broad bandwidth of the sensors, when utilized in conjunction with modern recording capabilities, offer the possibility to detect strain signals from a wide range of sources up to frequencies overlapping the passband of standard short-period seismic networks.

This report describes measurement of earth strain in the frequency band 10⁻⁸–10 Hz at a site about 1 km from the San Andreas fault zone near San Juan Bautista, California. Strain signals observed include earth tidal strains and superimposed seismic radiation fields generated by local earthquakes, teleseisms, and distant (493 km) nuclear explosions, and ground noise during seismically quiet times. A strain record of special interest was obtained at a hypocentral distance of 3.2 km in the near-source region of a local earthquake (M_L = 3.2). The broad bandwidth recording of the static and dynamic strain field for an event as small as this on the San Andreas fault represents a unique observation at frequencies up to 10 Hz and provides both an estimate of coseismic strain release and comparative source parameters estimated independently using simultaneous recordings from collocated seismometers.

Previous records of a coseismic strain offset have been obtained at an epicentral distance of 95 km for a larger mag-

nitude earthquake (M_L = 6.5) on the Imperial fault in southern California [Wyatt and Agnew, 1982]. However, these large earthquakes are very infrequent, and instabilities in surface instruments and near-surface materials [McHugh and Johnston, 1977] generally confuse surface observations. Offsets have also been recorded on borehole dilatometers for earthquakes on faults near Matsushiro, Japan [Sacks, 1979]. In these cases, the magnitudes ranged from M_L 3.4 to 4.8 km, but the hypocentral distances were larger (from 6.3 to 11 km). Measurement of the static field from the more frequent earthquakes on active faults at the M_L 3–5 level allows more rapid development of statistics of near-fault strain behavior and testing of models of fault rupture. At this point, only borehole strain instruments appear capable of recording static strain field changes reliably under conditions of high acceleration.

INSTRUMENTATION

The Sacks-Evertson dilational strainmeter used in this study [Sacks *et al.*, 1971] is installed at a depth of 138 m below the surface at a site, SRLS, about 1 km from the San Andreas fault (Figure 1). The sensors, installed as part of a cooperative program between the U.S. Geological Survey and the Carnegie Institution of Washington, are cemented in the borehole with expansive grout, having density characteristics approximating those of the granite host material. The borehole is then filled to the surface with cement to avoid long-term strains from hole relaxation effects and reequilibrium of the aquifer system.

Data from the instrument are routinely recorded on site with low-speed analog recorders (72-dB dynamic range from 0 Hz to 10 mHz) and are transmitted with a telephone line based 12-bit digital telemetry system (72-dB dynamic range

Copyright 1986 by the American Geophysical Union.

Paper number 5B5892.
0148-0227/86/005B-5892\$05.00

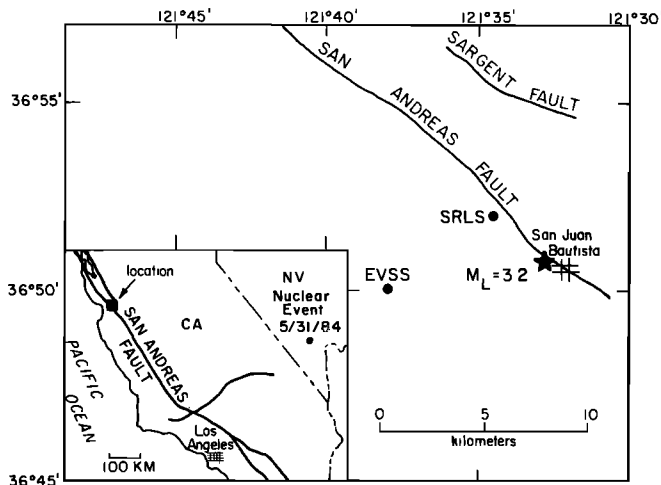


Fig. 1. Dilatometer sites EVSS and SRLS near San Juan Bautista, California, and the epicenter of a moderate earthquake (M_L 3.2) that occurred on May 26, 1984, at 0541 hours. The location of an underground nuclear explosion that occurred on May 31 is shown on the small inset general location map.

from 0 Hz to 1 mHz) at one sample every 10 min to Menlo Park, California [Rogers *et al.*, 1977]. The sensor and the telemetry system was calibrated using ocean-load corrected earth tides. Calibrations are repeatable to within 5%.

To extend the bandwidth and resolution of recorded strain data, wide dynamic range (16 bit; 96 dB), broad bandwidth (0–600 Hz) portable recorders (General Earthquake Observational Systems, or GEOS) were used to record simultaneous data from the strainmeters and collocated seismometers (1 Hz; Mark Products, L-4). The GEOS recorders, described by Borchardt *et al.* [1985], permit parameters such as gain (0–60 dB in 6-dB steps), anti-aliasing filters (7 pole Butterworth), sample rate (up to 1200 samples/s (sps)), and a variety of other parameters, to be selected on site. In this application, preset time, trigger, and continuous record modes have all been used to record the strain and simultaneous seismic signals in the bandwidth 0.0067– 10^5 s. Continuous recording mode with dc coupling and no low-cut filters was used to obtain continuous records of earth tidal strains with superimposed high-frequency seismic strain variations associated with seismic events and nuclear explosions over periods of 24–30 hours. The event triggering mode was used to record simultaneous seismic and strain data during several hundred local and distant earthquakes.

VOLUMETRIC STRAIN AND DISPLACEMENT FIELD FOR A P WAVE IN A VISCOELASTIC SOLID

To compare the P wave signals recorded on a dilational strainmeter with those recorded on a conventional three-component seismometer installation, we consider a P wave with a corresponding irrotational displacement field in a general homogeneous isotropic linear viscoelastic (HILV) solid, as described by Borchardt [1973]. A monochromatic P wave in a HILV solid is characterized by an expression of the form

$$\phi = B e^{i(\omega t - \mathbf{K} \cdot \mathbf{r})} \quad (1a)$$

with the complex wave vector given by

$$\mathbf{K} = \mathbf{P} - i\mathbf{A} \quad (1b)$$

and

$$\mathbf{K} \cdot \mathbf{K} = k_P^2 = \frac{\omega^2}{\alpha^2} = \frac{\omega^2 \rho}{\kappa + \frac{4}{3}M} \quad (1c)$$

where the material parameters ρ , κ , and M denote the density and the complex bulk and shear moduli, respectively [Borchardt, 1973]. Upon introduction of a rectangular coordinate system and consideration of a P wave with direction of propagation and maximum attenuation in the vertical (z) direction, the vertical component of the displacement field for a homogeneous P wave is given by

$$u_{Rz} = |Bk_P| e^{-\mathbf{A} \cdot \mathbf{r}} \cos[\zeta(t)] \quad (2a)$$

where

$$\zeta(t) = \omega t - \mathbf{P} \cdot \mathbf{r} + \arg[Bk_P] - \pi/2 \quad (2b)$$

The corresponding volumetric strain associated with the passage of a vertical traveling homogeneous P wave in a HILV solid can be obtained by differentiation of (2a) with respect to the spatial coordinate z and is given by

$$\Delta_R = |Bk_P| e^{-\mathbf{A} \cdot \mathbf{r}} |k_P| \cos\left[\zeta(t) - \left(\psi + \frac{\pi}{2}\right)\right] \quad (3a)$$

where k_P can be written in terms of the corresponding velocity and Q^{-1} for homogeneous waves as

$$|k_P| = \frac{\omega}{v_{HP}} \frac{(2\chi_{HP})^{1/2}}{(1 + \chi_{HP})^{1/2}} \quad (3b)$$

and

$$v_{HP}^2 = 2 \left(\frac{M_R}{\rho} \right) \frac{1 + Q_{HP}^{-2}}{1 + (1 + Q_{HP}^{-2})^{1/2}} \quad (3c)$$

$$\psi = \tan^{-1} \frac{Q_{HP}^{-1}}{1 + \chi_{HP}} \quad (3d)$$

$$\chi_{HP} = (1 + Q_{HP}^{-2})^{1/2} \quad (3e)$$

and subscripts H have been introduced to indicate restriction of the discussion to a homogeneous wave field. Consideration of inhomogeneous wave fields is beyond the scope of this manuscript. Equations (2) and (3) are valid for a general viscoelastic solid, independent of the amount of intrinsic absorption.

If we assume that the amount of intrinsic material absorption is small (i.e., low-loss materials for which $Q_{HP}^{-1} \ll 1$), then $\chi_{HP} \approx 1$, $|k_P| \approx \omega/v_{HP}$, and (2) and (3) show that the volumetric strain is scaled with respect to displacement by the familiar expression

$$|k_P| \approx \frac{\omega}{v_{HP}} \approx \frac{\omega}{(M_R/\rho)^{1/2}} \approx 2 \frac{\pi}{\lambda} \quad (4)$$

where λ represents wavelength. In addition, it can be easily shown that a minor phase shift occurs in volumetric strain due to the degree of anelasticity. Measurement of this phase shift could provide therefore an independent estimate of anelasticity in crustal materials.

For those situations in which the phase shift due to anelasticity is negligible, expressions (2) and (3) show that the velocity field, as detected on seismometers, and volumetric strain, as detected by a dilatometer, for one-dimensional propagation and attenuation are related by the simple amplitude scaling factor corresponding to the magnitude of the complex wave vector normalized by angular frequency as given by

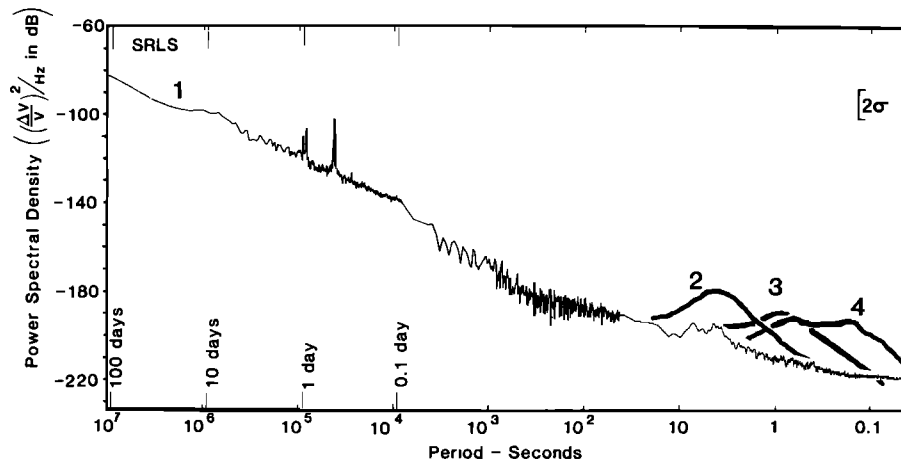


Fig. 2. Power spectral density for earth strain as determined at dilatometer site SRLS (Figure 1) for background earth strain (curve 1; 10^7 – 10^4 s from digital telemetry, 10^4 – 0.4×10^{-2} from GEOS); nuclear event detected by a dilatometer at a distance of 493 km (curve 2; 50 sps on GEOS), and a M_L 3.2 earthquake at a hypocentral distance of 3.2 km as simultaneously detected by dilatometer (curve 3; 50 sps on GEOS) and instrument-corrected seismometer (curve 4; 50 sps on GEOS). Curve 1 provides an estimate of earth strain over 8 orders of magnitude in period. Earth tidal strains (3×10^4 – 10^5 s) and microseisms (1–10 s) are clearly evident. Curves 2, 3, and 4 are smoothed strain spectra or equivalent strain spectra (curve 4; v_{HP}^{-1} scaling) and illustrate relative bandwidth detection capabilities for dilatometers and 1-Hz seismometers. Also shown are the 95% confidence limits for the spectral estimates.

$$\frac{|k_p|}{\omega} = \frac{1}{v_{HP}} \frac{(2\chi_{HP})^{1/2}}{(1 + \chi_{HP})^{1/2}} \quad (5)$$

which for low-loss media are approximately equal to $1/v_{HP}$.

OBSERVATIONS OF SHORT-PERIOD STRAIN

The first wide dynamic range digital recordings of earth strain and seismic data near the San Andreas fault were made during an 18-hour period on April 20, 1984, at a sensitivity, sampling rate, and gain of 5×10^{-11} , 50 sps (17-Hz anti-aliasing filter), and 42 dB, respectively. These data were initially used to develop estimates of earth strain noise in the period band 0.1– 10^4 s. The averaged noise spectrum in decibels referenced to 1 (strain)²/Hz, obtained from consecutive time series of 4000 data recorded at 50 sps and 0.08 sps, respectively, is shown in Figure 2. The spectrum decreases at about 10 dB per decade of frequency from –183 dB at a frequency of 0.001 Hz (1000 s) to –223 dB at 10 Hz. This spectral fall-off rate is consistent with that obtained at other sites [Johnston and Borchardt, 1984], and the overlapping spectral values agree within the errors. Microseismic peaks are apparent in Figure 2 between 4 and 8 s.

To investigate the recording quality with an expected short-period strain signal, a record of earth strain was obtained for a 28-hour interval at 10 sps with a gain of 42 dB during the detonation of a nuclear explosion in Nevada at 1945 hours on April 30, 1984 (Figure 3). The source and receiver locations, separated by a distance of 493 km, are shown in Figure 1 (inset). The high-frequency nuclear seismogram, superimposed on longer period earth tidal variations (Figure 3a), is plotted at a decimated sampling rate of 0.1 sps. Figures 3b and 3c show expanded time histories of the nuclear seismic radiation field simultaneously recorded as 10 sps by the strainmeter and a horizontal component velocity transducer on the ground surface. Because such high-quality wide band recordings of strain and ground velocity are rare for local earthquakes on the San Andreas fault, and because this information could

provide important details on the mechanism of failure, we attempted to obtain several similar records of the near-source strain and ground velocity fields of local earthquakes.

In the initial experiment the recorder was used during the time interval May 7 to May 29, 1984, as a four-channel system in event trigger mode to record simultaneous data at 50 sps from the dilatational strainmeter and three-component velocity transducers. Field calibration of the seismometers is described by Borchardt *et al.* [1985]. During the recording period, several tens of events were recorded. A shallow local earthquake of special interest occurred at a depth of 2.7 km, just to the south of SRLS on May 29, 1984 (hypocentral distance 3.2 km), when unfortunately, only one horizontal (east oriented) velocity transducer was in operation. The location of the earthquake, shown in Figure 1, was corrected for bias in routine locations caused by differences in seismic velocities on opposite sides of the fault zone [Engdahl and Lee, 1976]. Local magnitude (M_L 3.2), moment (6.3×10^{20} dyn cm) and source length (250 m) were determined using relations from Bakun [1984].

The seismic radiation from this vertically dipping strike-slip earthquake is clearly evident in the strain and ground velocity time histories shown in the upper and lower plots of Figure 4. Because the instrument location is just off strike (Figure 1), the east oriented seismic velocity transducer is well located to record both the P wave (50% of maximum amplitude) and S wave (90% of maximum amplitude) radiation fields of the earthquake [Kasahara, 1980]. Careful inspection of the strain record in the seconds before rupture indicates no precursory strain release above the resolution limit (5×10^{-11}). An offset is apparent in the strain seismogram and is more clearly seen when the record is low-pass filtered. The filtered version (dotted line in Figure 4) is shown superimposed on the strain time history on the upper plot in Figure 4. The filtered trace is consistent with the maximum offset of 1.86 nanostrain occurring at, or just after, the arrival of the S wave. No such offset is apparent, nor would be expected, on the simulta-

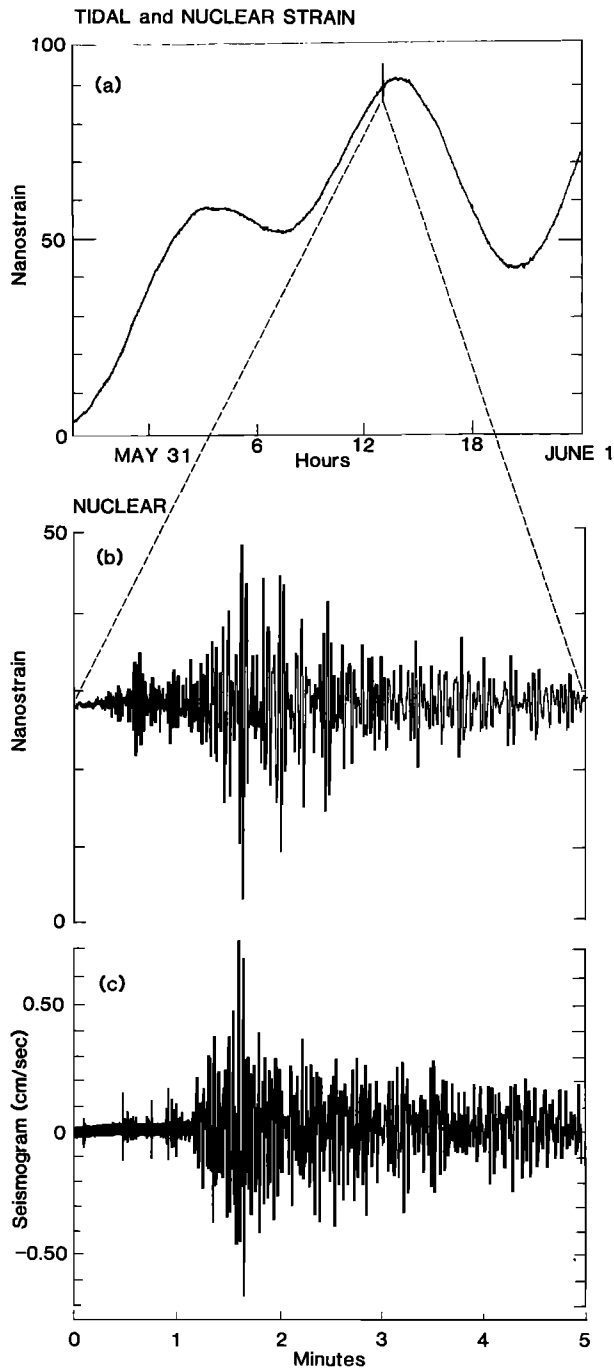


Fig. 3. (a) Dilational strain recorded by the Sacks-Evertson dilatometer and ground motion variations detected by a seismometer on May 31 at a gain and sample rate on a GEOS recorder of 42 dB and 10 sps, respectively. The upper strain time history plotted for a 28-hour intervals at 0.1 sps shows earth tidal strain and strain associated with the detonation of an underground nuclear explosion in Nevada at a distance of 493 km. (b) The second time history plotted at 10 sps shows an expanded version of the strain variations recorded from the nuclear explosion. (c) The third time history plotted at 10 sps represents the ground motion recorded from the nuclear explosion as detected simultaneously by a horizontal velocity transducer at the ground surface.

neously recorded seismogram from the horizontal velocity transducer.

The earthquake was modeled (Figure 5) as failure on a patch of the fault with a final dimension 250×250 m, cen-

tered at a depth of 2.6 km. The quasistatic dislocation model used allows the failure patch to grow with time, with either or both strike-slip and dip-slip displacement, although only strike-slip was used in this case. A rigidity of 2.3×10^5 bars was assumed, and for a moment of 6.3×10^{20} dyn cm, the slip predicted for the event is 4.4 cm. Assuming plane stress conditions, the perturbation in dilational strain is 1.66×10^{-9} in the same sense as the 1.86×10^{-9} observed. Uncertainties in the values of the various fault zone parameters imply at least a factor of 2 uncertainty in the calculated strain offset value.

From the records for the M_L 3.2 earthquake, smoothed versions of the strain power density spectrum computed from the strain seismogram, and equivalent strain power density spectrum computed from the velocity seismograms, are shown in Figure 2. The spectrum from the velocity transducer is corrected for instrument response and is scaled to strain by $1/v_{HP}$. It is evident that most of the energy detected by the strainmeter is in the period band 0.1–10 s, with a peak at about 1 s, whereas that detected by the seismometer peaks at about 0.6 s. Within the 95% confidence limits (13 dB), the two

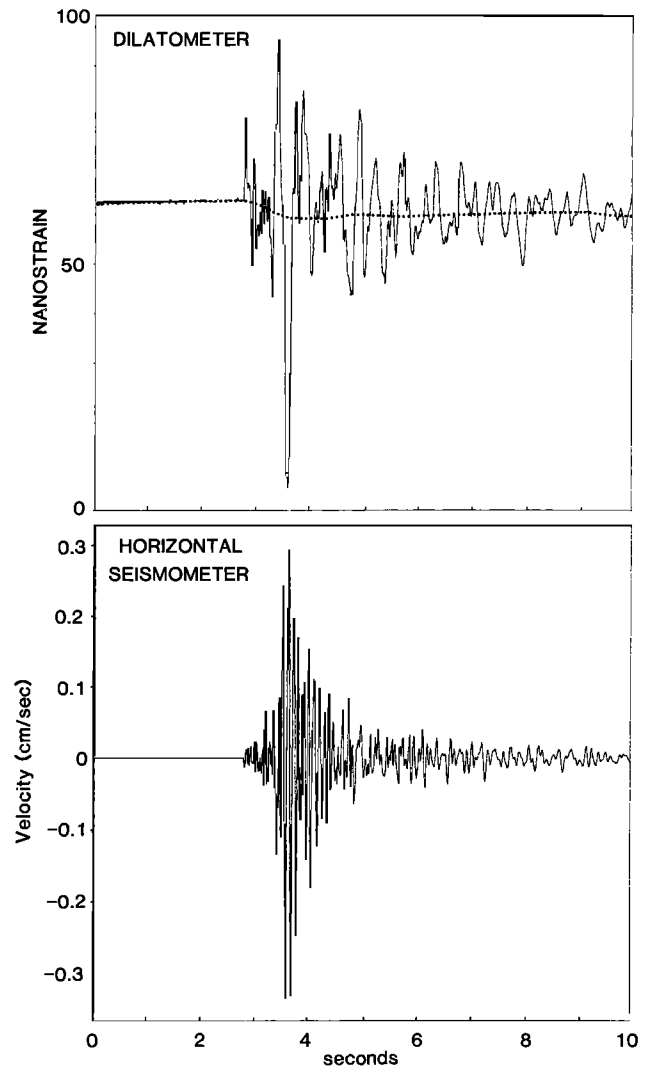


Fig. 4. Comparative volumetric strain and horizontal seismometer records obtained on GEOS at a hypocentral distance of 3.2 km during a local earthquake M_L 3.2 at 0541 on May 26, 1984. The velocity transducer was oriented in an east-west direction (east displacement positive).

MODEL OF SAN JUAN BAUTISTA EARTHQUAKE
($M_L=3.2$) MAY 26, 1984

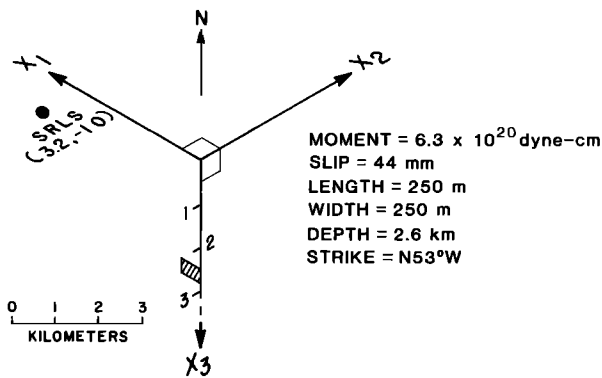


Fig. 5. Dislocation model used to calculate the expected strain step from the May 29, 1984, magnitude 3.2 earthquake. The parameters chosen are discussed in the text.

spectra agree at frequencies below 1 Hz. Because of the poor low-frequency response characteristics of the velocity transducer, energy at periods greater than 5 s is not well determined. The wide dynamic range of the dilatational strain transducer is clearly evident.

Equivalent displacement spectra were calculated from the complete time histories from each sensor (see Figure 4) after the record from the seismometer was first corrected for the response of the L-4 transducer using a program by C. Mueller. Here, $v_{HP}/\omega = \lambda/2\pi$ scaling was used to transform the strain spectrum into a displacement spectrum, and ω^{-1} scaling was used to transform the velocity spectrum also into a displacement spectrum, where v_{HP} is taken to be 3 km/s [Bakun and McLaren, 1984]. The results obtained are shown in Figures 6a and 6b. Within the estimated uncertainties, the two spectra agree at frequencies below 1 Hz. The least count noise level corresponding to about 5×10^{-11} in strain for a gain of 6 dB in the GEOS is shown as a dashed line on the strain displacement spectrum.

The increased bandwidth of the strainmeter at long periods is evident in the spectrum derived from the strain data (Figure 6b), with the majority of the seismic energy detected occurring at frequencies between 15 and 0.1 Hz (0.06–10 s). In contrast, most of the seismic energy detected by the velocity transducer occurs between 20 and 0.5 Hz. In situ calibration of the L-4 velocity transducer [Borcherdt et al., 1985] shows that the transducer is linear in this range and that seismic signals at frequencies less than 0.1 Hz generally cannot be resolved. At frequencies just above 10 Hz, the strain displacement spectrum approaches the background earth strain noise level (see Figure 2), which is just above the least count noise level at 6-dB gain chosen for the recorder. The response of the strainmeter decreases at high frequency because of internal hydraulic filtering [Sacks, 1979]. Records of ground strain noise taken at higher gains and 100-Hz sampling with a 33-Hz anti-aliasing filter show high-frequency roll-off between 20 and 30 Hz. Some of this roll-off may be due to hydraulic filtering and some due to the effects of the 33-Hz anti-aliasing filter. Across the frequency band where the disagreement in spectral amplitudes occurs, the strainmeter has a linear response.

The two near-field ground displacement spectra indicate that the corner frequency f_c [Brune, 1970] is distinctly different in the two records. From the strain transducer the inferred

corner frequency f_c is about 1 Hz, whereas that inferred from the velocity transducer is about 5 Hz. If correct, this implies significantly different estimates of source parameters obtained from near-field recordings on the surface compared with those obtained from recordings more than 100 m beneath the surface. To investigate this issue, comparative corner frequencies were computed from a set of 10 more distant events (not shown here) with similar strain and velocity amplitudes that were simultaneously recorded on the deep strain transducer and the same velocity transducer at the surface. For these events, f_c , as determined from equivalent ground displacement spectra from horizontal velocity and strain data, are generally similar. Thus only the data sets obtained from the two sensor types in the near field of this M_L 3.2 earthquake have shown significant differences in f_c in their corresponding ground displacement spectra.

DISCUSSION

The wide dynamic range of recently installed Sacks-Evertson borehole strainmeters, when used with wide dynamic range broadband recorders, permits detection of strain signals to 96 dB above the present resolution limit of the strainmeter ($< 10^{-11}$). The bandwidth with the strainmeter capacitor coupled to the GEOS channel is presently about 10^{-4} –10 Hz. This allows on-scale recordings for the large-amplitude dynamic strain fields expected from moderate to large earthquakes as well as recordings of the more frequent smaller local

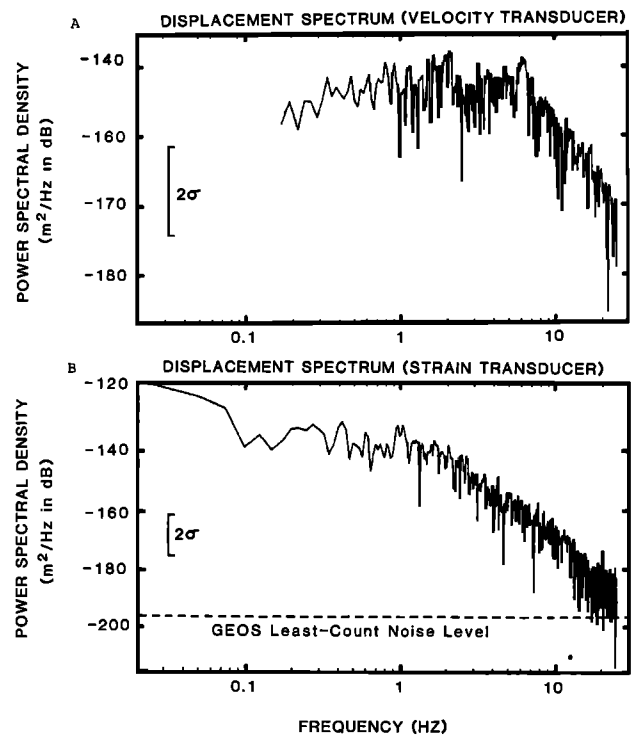


Fig. 6. (a) Ground displacement spectrum and 95% confidence limits (13 dB) determined from the seismic velocity time history shown in Figure 4. (b) Ground displacement spectrum and 95% confidence limits (13 dB) determined from the strain time history shown in Figure 4. To avoid bias at low frequencies, the static step shown in Figure 4 was removed before the spectrum was determined. The GEOS least count noise level at 6-dB gain is shown as a dashed line. Comparison of the spectra demonstrate the improved long-period detection capabilities of the dilatometer in comparison with conventional short-period seismometer and an apparent difference in inferred corner frequency (see text).

events on the San Andreas fault. Statistics on source parameters can be rapidly accumulated from these more frequent events in the range M_L 3–4.

The level and characteristics of earth strain noise estimated from the SRLS site suggest strain signals as low as 5×10^{-11} can be detected in the period range 0.1–10 s, while for the passband 10–10⁴ s the strain detection level is from 10^{-10} to 10^{-9} . This latter passband, which is clearly outside that of regional seismic networks and conventional strong-motion instrumentation, is of considerable interest for a variety of studies, especially those on rupture initiation and earthquake prediction. The expressions describing the volumetric strain scalar and the vector displacement field for irrotational body waves in a general linear viscoelastic solid suggest methods whereby data from colocated seismometers and strainmeters might be used to estimate anelastic properties of crustal materials that could not be inferred from data recorded on either sensor alone.

A rare near-source recording of a local event on the San Andreas fault suggests coseismic strain release is generally consistent with simple dislocation models of the event. Additional events recorded at other sites in the near-source region are needed to quantify further the behavior reported here. Several other instruments, including a three-component borehole strainmeter [Gladwin, 1984], were operating in the vicinity of the May 26 earthquake, but because of the slow sample rate (one sample every 15 min), it was difficult to obtain independent measurements of the few nanostrain offsets expected on these instruments.

Offsets have been observed on dilatometers during seismic events induced by mine operations in South Africa [McGarr *et al.*, 1982] and during the Matsushiro earthquake swarm in Japan [Sacks, 1979]. Without correction for the focal mechanisms of the events, McGarr *et al.* [1982] showed that the observed amplitudes agreed within a factor of 10 with those expected from simple point source dislocation models of the events. Analysis of high-quality recordings of the right-lateral strike-slip event on May 26, where both focal parameters and hypocentral distance were known, permitted a more complete comparison between observation and a simple model of the event derived from elastic dislocation theory.

The simultaneous detection of the near-source radiation field of this earthquake by the borehole strainmeter and a surface seismometer allowed a preliminary comparison of the inferred source parameters. Displacement spectra, determined independently for the event from the strain and velocity data, indicate that the apparent corner frequency f_c , as defined by Brune [1970], is distinctly different in each spectrum. The velocity transducer indicates an f_c of about 5–6 Hz, whereas on the strain transducer, f_c is between 1 and 2 Hz. This would imply correspondingly different estimates of source size and stress drop. In situ calibration of the velocity and strain transducers suggests that this discrepancy is not explained by variations in instrument linearity. Since displacement spectra determined from the same sensors for more distant events with near-vertical angles of incidence are in general agreement, the most likely explanation is that the surface seismic observations for the May 26 event are contaminated by amplification effects in the low-velocity near-surface materials that are stimulated at the particular angle of incidence for this earthquake. Cranswick *et al.* [1985] have independently pointed out that near-surface ground response effects can bias source parameter estimates. More simultaneous measurements of near-field radiation on colocated borehole sensors within a few kilometers of the rupture nucleation point should test

near-field source parameter determinations more thoroughly and define the influence of near-surface low-velocity materials on surface observations.

Acknowledgments. The dilatometers were installed as part of a cooperative program between the U.S. Geological Survey and the Carnegie Institution of Washington. Selwyn Sacks, Mike Seeman, Glen Poe, Doug Myren, Jack Healy, and others participated in the installation and provided technical support. The GEOS development, field operations, and data retrieval result from dedicated contributions by G. Maxwell, G. Jensen, J. VanSchaack, J. Fletcher, R. Warrick, R. McClearn, D. Myren, J. Sena, J. Gibbs, J. Watson, and C. Dietel. Software developed by G. Maxwell was used to read GEOS tapes, with software developed by J. Herriot, E. Cranswick, and S. Silverman used to display and process the data. C. Mueller and L. Haar kindly provided independent estimates of displacement spectra and f_c , respectively, for several events. Bill Bakun, Paul Spudich, and an anonymous reviewer made useful comments on the paper.

REFERENCES

- Bakun, W. H., Seismic moments, local magnitudes, and coda-duration for earthquakes in central California, *Bull. Seismol. Soc. Am.*, **74**, 439–458, 1984.
- Bakun, W. H., and M. McLaren, Microearthquakes and the nature of the creeping-to-locked transition of the San Andreas fault zone near San Juan Bautista, California, *Bull. Seismol. Soc. Am.*, **74**, 235–254, 1984.
- Borcherdt, R. D., Energy and plane waves in linear viscoelastic media, *J. Geophys. Res.*, **78**, 2442–2453, 1973.
- Borcherdt, R. D., J. B. Fletcher, E. G. Jensen, G. L. Maxwell, J. R. VanSchaack, R. E. Warrick, E. Cranswick, M. J. S. Johnston, and R. McClearn, A general earthquake observation system (GEOS), *Bull. Seismol. Soc. Am.*, **75**, 1783–1826, 1985.
- Brune, J. N., Tectonic stress and spectra of seismic shear waves from earthquakes, *J. Geophys. Res.*, **75**, 4997–5009, 1970.
- Cranswick, E., R. Wetmiller, and J. Boatwright, High-frequency observations and source parameters of microearthquakes recorded at hard rock sites, *Bull. Seismol. Soc. Am.*, **75**, 1535–1568, 1985.
- Engdahl, E. R., and W. H. K. Lee, Relocation of local earthquakes by seismic ray tracing, *J. Geophys. Res.*, **81**, 4400–4406, 1976.
- Gladwin, M. T., High precision multi-component borehole deformation monitoring, *Rev. Sci. Instrum.*, **55**, 2011–2016, 1984.
- Johnston, M. J. S., and R. D. Borcherdt, Earth strain in the period range 0.1–10,000 seconds at six borehole sites within the San Andreas fault system, *Eos Trans. AGU*, **65**, 1015, 1984.
- Johnston, M. J. S., A. T. Linde, I. Sacks, and D. Myren, Borehole dilatometer strain array—Installation and preliminary results from the Mojave Desert, *Eos Trans. AGU*, **63**, 430, 1982.
- Kasahara, K., *Earthquake Mechanics*, 248 pp., Cambridge University Press, New York, 1980.
- McGarr, A., I. S. Sacks, A. T. Linde, S. M. Spottiswoode, and R. W. Green, Coseismic and other short-term strain changes recorded with Sacks-Evertson strainmeters in a deep mine, *Geophys. J. R. Astron. Soc.*, **70**, 717–740, 1982.
- McHugh, S., and M. J. S. Johnston, An analysis of coseismic tilt changes from an array in central California, *J. Geophys. Res.*, **82**, 5692–5697, 1977.
- Rogers, J., M. J. S. Johnston, C. E. Mortensen, and G. D. Myren, A multichannel digital telemetry system for low-frequency geophysical data, *U.S. Geol. Surv. Open File Rep. 77-490*, 1977.
- Sacks, I. S., Borehole strainmeters, Proceedings Conference on Stress and Strain Measurements Related to Earthquake Prediction, *U.S. Geol. Surv. Open File Rep. 79-370*, 425–485, 1979.
- Sacks, I. S., S. Suyehiro, D. W. Evertson, and Y. Yamagishi, Sacks-Evertson strainmeter, its installation in Japan and some preliminary results concerning strain steps, *Pap. Meteorol. Geophys.*, **22**, 195–207, 1971.
- Wyatt, F., and D. Agnew, Strain and tilt offsets from an earthquake in southern California, *Eos Trans. AGU*, **63**, 375, 1982.

R. D. Borcherdt and M. J. S. Johnston, U.S. Geological Survey, 345 Middlefield Road, MS/977, Menlo Park, CA 94025.

A. T. Linde, Carnegie Institution of Washington, Washington, D. C. 20015.

(Received December 6, 1985;
revised May 29, 1986;
accepted July 7, 1986.)